Effects of Unloading-Reloading History on Pullout Resistance Related to Soil Dilatancy and Geogrid Properties

Giang H. Nguyen, Department of Civil & Environmental Engineering, Saitama University, JAPAN, s07de054@mail.saitama-u.ac.jp
Jiro Kuwano, Department of Civil & Environmental Engineering, Saitama University, JAPAN, jkuwano@mail.saitama-u.ac.jp
Jun Izawa, Department of Civil Engineering, Tokyo Institute of Technology, JAPAN, jizawa@cv.titech.ac.jp
Sakae Seki, Department of Civil Engineering, Tokyo Institute of Technology, JAPAN, jizawa@cv.titech.ac.jp

ABSTRACT**:**
In order to understand about mechanism of pullout test under seismic activities, unloading-reloading process is applied to simulate the geogrid being pushed back and forth under earthquakes. Different geometry of geogrids exhibits influence of soil dilatancy, geogrid's opening, distance between transverse ribs on pullout resistance. In this research, square and circle geogrid types are tested. Results reveal that unloading-reloading decreases pullout resistance of geogrid at the peak values and at the residual parts due to the soil dilatancy effect however it has little impact before the peaks. The reductions of pullout resistance are differed with different types of geogrid during shearing. At peak values, soil shows the most dilative and contractive behaviors however, at the residual part soil just shows the contractive behavior under the unloading-reloading process. This study will help to evaluate degree of damage in the geogrid reinforced soil walls after earthquakes.

1. INTRODUCTION

Geogrid reinforced soil walls (GRSW) are often used without considerable repair or reconstruction after simple inspection in many cases even after strong earthquakes. For the proper repair or reconstruction, it is necessary to evaluate damage of GRSW. As the restoration method of the structure should be decided right after the event, the damage must be evaluated by a simple index such as the wall displacement, the crest settlement, soil-geogrid interaction conditions. In order to properly understand mechanism of geogrid reinforced-soil under seismic activities, properties and tensile stiffness of geogrid, unloading-reloading process, which is applied to simulate geogrid being pushed back and forth under earthquakes, are studied.

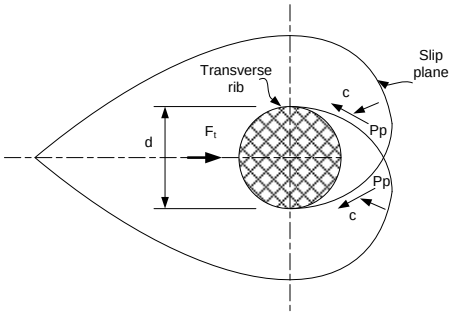

Figure 1. Failure plane for bearing resistance after Peterson and Anderson (1980)

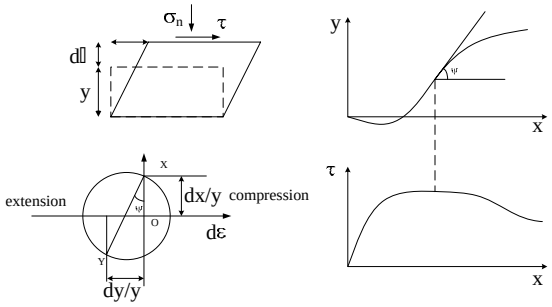

Figure 2. Dilatancy angle at peak values (Yasufuku & Ochiai, 2004)

Stress distribution along reinforcement contains two components, frictional resistance and passive resistance. The frictional resistance depends on the surface area between geogrid and soil, the friction angle between geogrid and soil, and effective normal stress at the interface (Bergado et al.,1992). The passive resistance is considered similar to bearing capacity mechanism. The failure mechanism is based upon the Terzaghi-Buisman bearing capacity equation for a strip footing as mentioned by Colin J. F. P. Jones (1996). Peterson and Anderson (1980) provided a bearing capacity failure mechanism shown in Figure 1. Passive resistance depends on area of transverse elements, effective vertical stress and friction angle of soil. However, experiment has shown the existence of confining effect which is independent of tensile force of geogrid. The confining effect is a factor of reinforcing effects related to soil dilatancy. Yasufuku and Ochiai (2004) reported an existence of confining effect in an element test, Figure 2.

In this study, a special pullout test is designed to carry out the pullout test with different geogrid types. The square and circle geogrid types are tested. To understand and stimulate geogrid working mechanism under seismic activities, unloading-reloading is applied during the pullout test by pushing the geogrid back and forth. The interaction between geogrid and soil especially at the transverse ribs is analyzed by the Particle Image Velocimetry (PIV) method to understand about the dilatancy mechanism during unloading-reloading process.

2. TEST APPARATUS

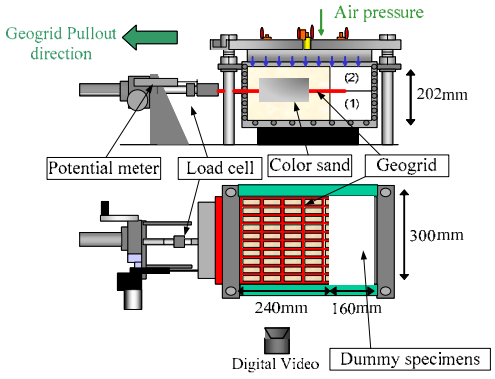

Figure 3. Mark 2 pullout test apparatus

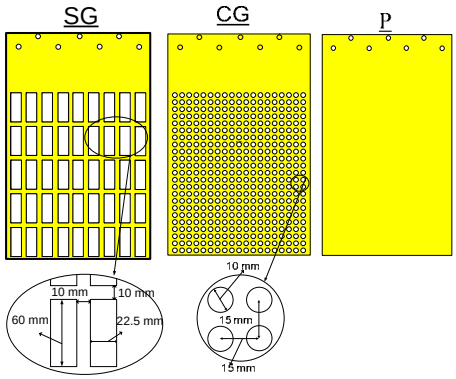

Figure 4. Polycarbonate types

Figure 3 shows the schematic diagram of Mark 2 pullout test apparatus with dimensions of 300 mm (width) x 202 mm (height) x 400 mm (length). Two dummy specimens are put inside the box to reduce frictional area between geogrid and soil making the contact length be 240 mm. The test apparatus is mainly made of steel except the longitudinal sidewalls which are made of hard transparent plastic plates. Color sands are glued at the observation square at the box side with an area of 134 mm (width) x 80 mm (height), distance from left side of the box to the square is 30 mm, to observe the deformation at the interface between geogrid and sand by a digital video camera. Dry Toyoura sand is poured through multiple sieves to make soil homogeneous and the density (D_r=80%) is controlled by the dropping vertical height, 170 mm, above the surface. As sand reaches the middle level of the box, geogrid is placed then sand is continued to be poured until reaching the top of the box. Air pressure bag is used to apply a constant uniform vertical pressure from the top of the box. The tests are operated by pulling the geogrid out at a constant speed of 1 mm/min through a screw jack controlled by a motor. The pullout force is measured by a tension load cell. Pullout displacement of geogrid is measured by a displacement gauge. All readings are automatically scanned and stored at four second intervals by an electronic data acquisition system. Two types of geogrid made of polycarbonate, a square geogrid (SG), a circle geogrid (CG) and a polycarbonate plate are shown in Figure 4. The results of tensile test of these geogrids were summarized in Table 2. The pullout tests were finished at 55 mm because of the limitation in the stroke of the jack.

3. MATERIAL

Toyoura sand which has the properties as shown in the table 1 is used in this study.

Table 1. Properties of Toyoura sand

D_{50} (mm)	U_c	e_{max}	e_{min}	e	ϕ (°)
0.19	1.56	0.973	0.609	0.682	43

Two types of geogrid made of polycarbonate, a square geogrid, a circle geogrid and a polycarbonate plate are shown in Figure 4.

Tests are carried out with two kinds of loading processes, no unloading-reloading (NUR) process and with 3-time unloading-reloading (UR) process at different loading level, under three different overburden pressures σ_v of 5 kPa, 20 kPa and 35 kPa

Table 2. Properties of model geogrid for unloading-reloading test

Square geogrid		
Thickness	mm	1.0
Pitch between transverse ribs	mm	70.0
Pitch between longitudinal ribs	mm	32.5
Width of the transverse rib	mm	10.0
Width of the longitudinal rib	mm	10.0
Tensile strength	(kN/m)	20.2
Circle geogrid		
Thickness	mm	1.0
Diameter	mm	10.0
Pitch between transverse ribs	mm	15.0
Pitch between longitudinal ribs	mm	15.0
Tensile strength	(kN/m)	85.6

5. RESULTS AND DISCUSSIONS

5.1 No Unloading-Reloading Process

Figure 5 a, b, c show pullout test results with no unloading-reloading step under different overburden pressures. The pullout resistance gradually reaches the peak value and then decreases in all the cases. In this study the circle geogrid is stiffer than the square geogrid. From the pullout resistance it can be observed that the square geogrid needs a big displacement to reach to the peak values however the other two which are stiffer than square one showed the peak pullout resistance at the small pullout displacement to mobilize the peak pullout resistance.

The pullout resistance of the circle geogrid shows clear shape around the peak values in compare with those of square and plate ones. The $\tan\delta_p / \tan\phi$, the ratio of the internal friction angle of soil itself and pullout

friction angle are from circle geogrid, square geogrid and plate respectively in large orders as seen in Figure. 5d.

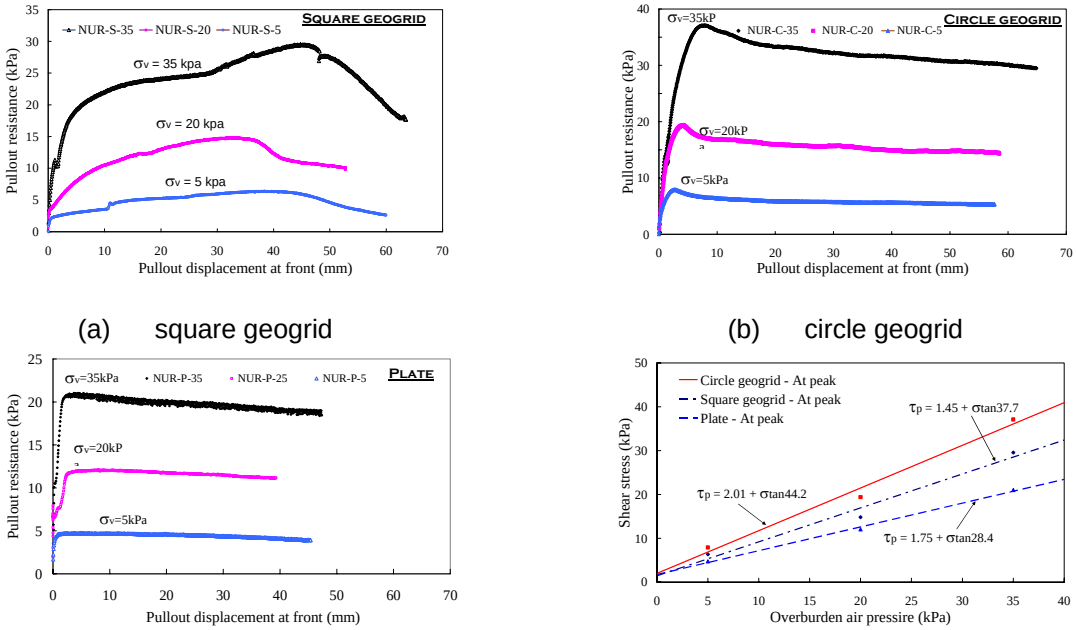

(a) square geogrid (b) circle geogrid

(c) plate (d) shear stress at peak values

Figure 5. Pullout test results with no unloading-reloading step

5.2 Unloading-Reloading Process

The unloading-reloading steps are implemented at 3 stages: before the peak value, at the peak value and at the residual part (Figure. 6 a, b, c). The whole process is presented through successive steps: O-A-B-C-D-E-F-G-H (for example, σ_v = 35 kPa). To achieve zero pullout resistance in unloading, the geogrid is pushed back slightly at the jack. Unloading-reloading process before the peak values is O-A-B-C. The process at the peak value is C-D-E and one more time at the residual part is F-G-H. Reduction in pullout resistance before and after unloading-reloading process, e.g. τ_b at C and τ_r at E in Figure 6, in the form of $(\tau_b - \tau_r)/\tau_b\,(\%)$. In these tests, the decreases at peak value of CG, SG and plate were 5%, 10% and 5% respectively.

Before the peak values, the UR does not affect the pullout resistance however it does reduce the pullout resistance at the peak and residual parts. It can be explained that before the peaks the shear band along the geogrid has not been formed therefore a disturbance by unloading-reloading does not change the shear resistance. But once the shear band is formed, the UR disturbs the boundary leads to the reduction of pullout resistance.

As the frictional resistance is similar during the unloading-reloading process, the reduction in the pullout resistance can be explained by the bearing interaction mechanism occur at both the node embossment and the transverse ribs and soil dilatancy. Soil dilatancy or confining effect is the effect of restriction of soil around the geogrid by the geogrid during the shearing. The confining effect increases the confining stress around geogrid. Restriction of soil is affected by the pitch between transverse ribs, stiffness of transverse elements and node embossments.

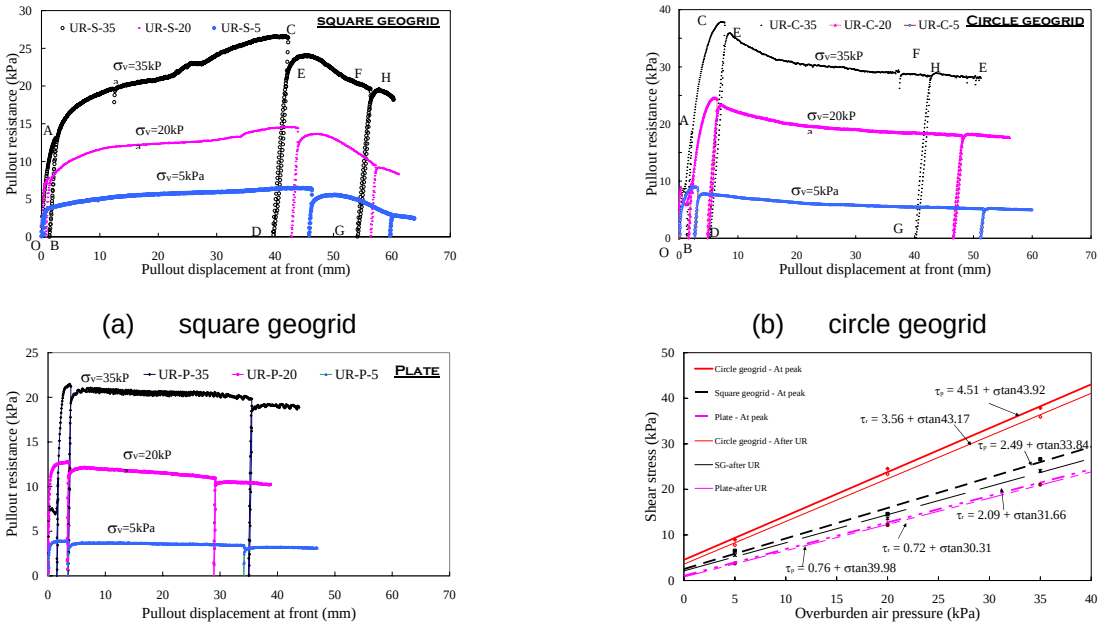

(a) square geogrid (b) circle geogrid

(c) plate (d) shear stress at peak

Figure 6. Pullout test results with unloading-reloading step

5.3 PIV and Soil Dilatancy Analysis

The interaction between geogrid and soil especially at the transverse ribs is analyzed by the Particle Image Velocimetry (PIV) method to understand about the dilatancy mechanism during unloading-reloading process. The color area is captured by a digital camera. Images are studied about the movement of sand around the geogrid. The interaction between soil and geogrid includes frictional resistance, passive resistance and confining effect. The whole unloading-reloading procedure with σ_v = 35 kPa and circle geogrid is analyzed and shown in the Figure 7. It can be seen that soil deforms most at the peak value (B→C) at the upper part as shown in red and yellow colors. The lower part shows just less deformation in compare with the upper part. It is due to the boundary condition of the test apparatus. The upper part is the stress boundary by the air bag therefore the deformation is not restricted. But the lower part of the box has a rigid boundary that restricts the deformation of soil.

Figure 8 shows x and y direction displacement analysis of the 1st row of the observed area. Δx denotes a displacement increment in x-direction from the previous step, e.g. Δx_c is Δx from B to C. If the value of Δx is positive then it means the soil particle moves in the same direction as a pullout direction. If Δx is negative, the soil particle moves in the opposite direction to a pullout direction. Δy indicates a displacement increment in y-direction from the previous step. If Δy is positive then it means the soil particle moves upward and soil shows volume increase or dilative behavior. If Δy is negative, the soil particle moves downward and soil shows volume decrease or contractive behavior.

E.g.

$$\Delta x_A = x_A - x_O$$
$$\Delta x_B = x_B - x_A \qquad [1]$$

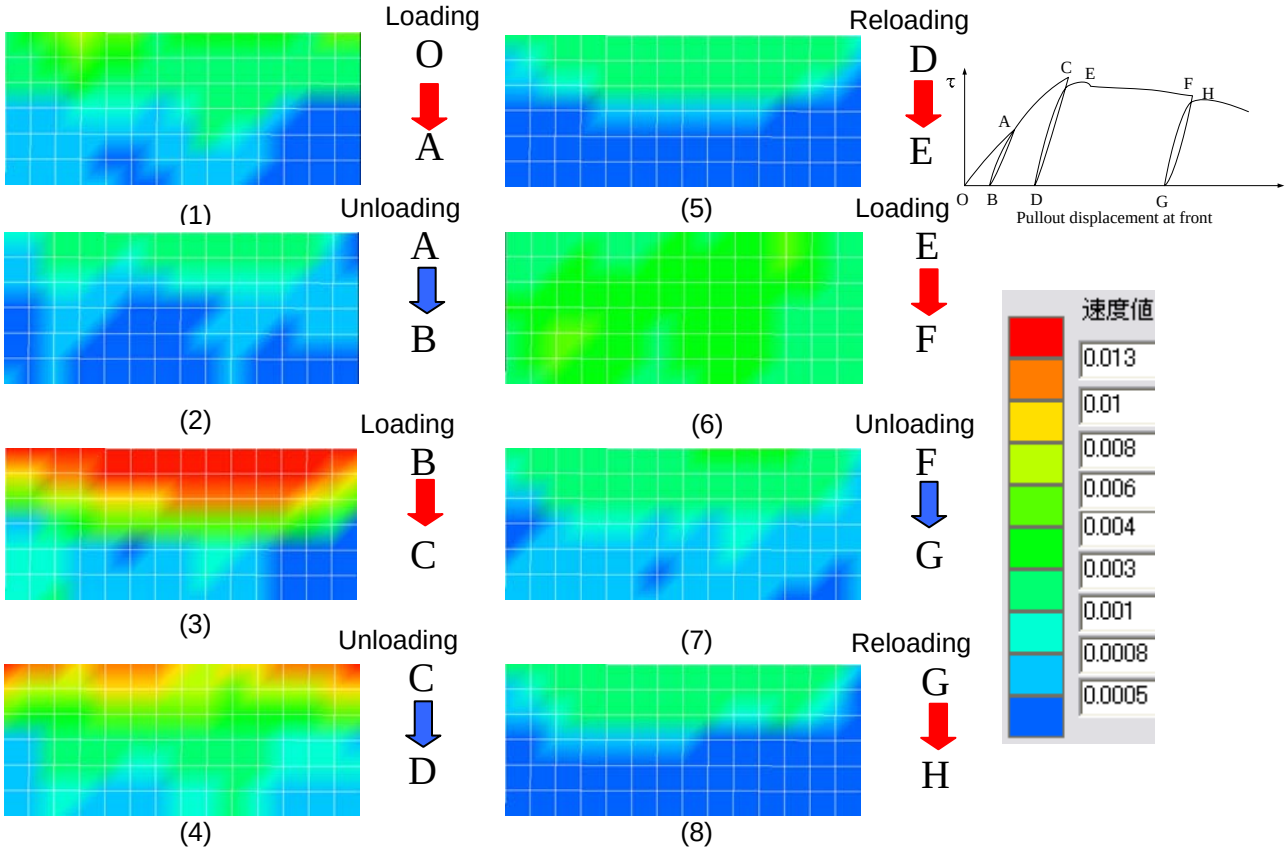

Figure 7. Deformation of soil around geogrid with unloading-reloading; $\sigma_v = 35$ kPa; Circle geogrid

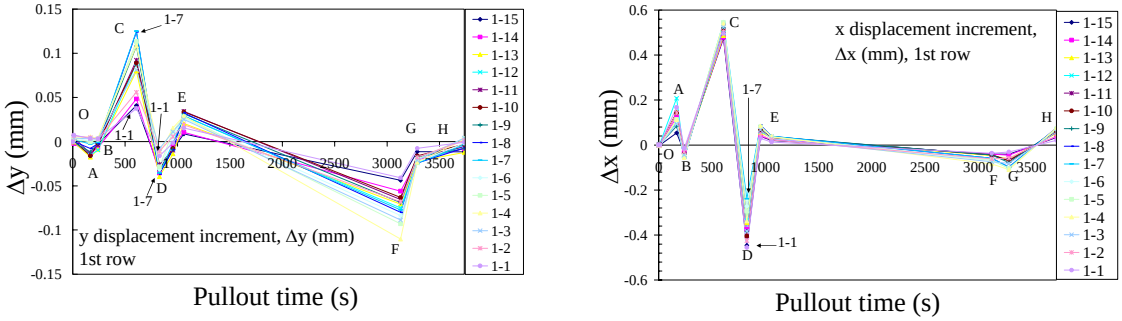

a) Increment of soil particle in y-direction

b) Increment of soil particle in x-direction

Figure 8. Increments of particles from O~H steps, Unloading-Reloading process, 35 kPa

As shown in Figure 8b on Δx, it is observed that from O→A, when geogrid is pulled out to the left soil particle move also to the left with the geogrid. When unloaded from A→B, geogrid is pushed back to the right and the soil particles also move to the right. Soil particles show large displacements in the pullout direction to the peak, C. At peak, unloading step pushes soil particles a big displacement toward the opposite pullout direction (from C→D). After peak, the shear zone is formed around geogrid's surfaces therefore soil particles show small displacement even under unloading-reloading process (F to G).

In the Δy graph of Figure 8a, soil shows contractive behavior at the beginning as values of Δy at A and B are negative. However at peak C, soil shows the most dilative behavior. These are similar to the soil dilatancy behavior as reported by Yasufuku & Ochiai (2004) in Figure. 2. In unloading step from C→D, soil shows contraction. During reloading, D→E, soil also shows volume increase until E however the volume increase rate is less than that up to C. In the residual state, once the shear zone is formed, soil just shows contractive behavior even under unloading-reloading process.

It can be observed in the y-direction graph of Figure 8 that the volume changes at C show more variation among the observed points 1-1~15 than those at D. Data for particles 1-7 and 1-1 are identified in Figure 8 to examine their behavior. The particle 1-7 is in front of a transverse rib and particle 1-1 is behind a transverse rib. When loaded, soil particles in front of transverse elements are restricted and pushed by the transverse elements due to bearing resistance. Soil particles behind transverse elements are less affected by this mechanism therefore particle 1-7 shows more dilative behavior than the particle 1-1 does. The soil particle 1-7 is in the passive zone and particle 1-1 is in the active zone due to bearing resistance of transverse elements. Particle 1-7 therefore is selected to have further evaluation in Figure 9 a, b, c.

5.4 Circle geogrid results

Figure 9 a & b are x and y displacements of observed point of 1-7 in a pullout test on a circle geogrid under σ_v =35 kPa. From these data, Figure 9c is drawn to show an x-y displacement trajectory of particle 1-7 throughout the pullout sequence. Soil around the peak C shows the largest dilatation however after the unloading-reloading the amount of dilatation at E is less than that at the peak therefore it leads to the less confining effect. This explains why unloading-reloading decreases the pullout resistance.

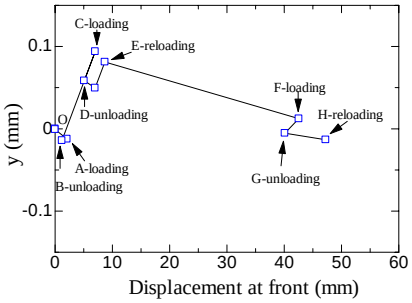

a) x displacement against time

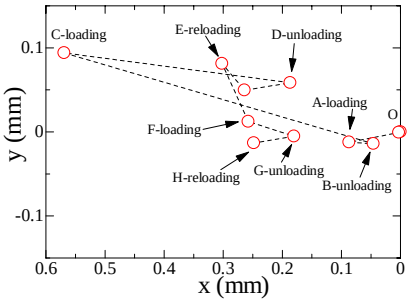

b) y displacement against time

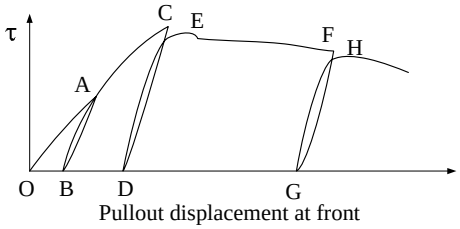

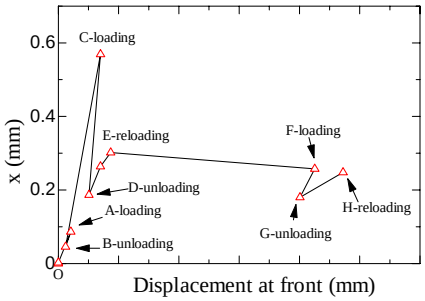

c) Particle 1-7 position in x & y coordinate

Figure 9. Soil particle's positions during shearing with unloading-reloading; circle-geogrid; 35kPa

6. CONCLUSIONS

Study on the pullout resistance was made on the model geogrids. Special attention was directed to see the effects of the shape and stiffness of geogrids and confining effect during unloading-reloading process.

The followings were obtained in this study

1. The unloading-reloading reduces pullout resistance at the peak and residual part due to soil dilatation however it shows very little effect before peak
2. Soil contracts at the beginning and then dilates most at the peak value during shearing.
3. Unloading-reloading pushes soil particles move a long distance at the peak value however after the shear zone is formed soil particles show small deformation.
4. The unloading-reloading reduces the confining effect leading to the decrease of pullout resistance
5. Soil at the upper part of pullout box deforms more than that of the lower part due to the boundary conditions.

ACKNOWLEDGEMENTS

This work has been done as a part of research project sponsored by Monbu Kagakusho Scholarship & Grant-in-Aid Scientific Research No.20360208. Assistance and facilities provided by the Department of Civil Engineering, Tokyo Institute of Technology (TIT), Japan is greatly appreciated.

REFERENCES

Yasufuku, N., Ochiai, H., Kaneshige, M., Kawamura, T. and Hirai, T. (2004) “Confining effect in geogrid-reinforced soil related to soil dilatancy” Proceeding, GeoAsia2004, Seoul, Korea: 385-394

Dennes T. Bergado, Kam-Hung Lo, Jin-Chun Chai, Ramaiah Shivashankar, Marolo C. Alfaro, Loren R. Anderson (1992) “Pullout test using steel grid reinforcements with low-quality backfill”, Journal of Geotechnical Engineering, ASCE, 118: 1047-1062

Peterson, L. M., Anderson, L. R. (1980). “Pullout resistance of welded wire mats embedded in soil” M Sci. Thesis, Utah State Univ., Logan, Utah.

Colin J. F. P. Jones (1996) “Earth reinforcement and soil structures” Thomas Telford, London, England